

# A Raman and photoconductivity analysis of boron-doped SiC:H films deposited using the electron cyclotron resonance method

S. F. YOON, R. JI, J. AHN

*School of Electrical and Electronic Engineering, Nanyang Technological University, Nanyang Avenue, Singapore 639798, Republic of Singapore*

W. I. MILNE

*University of Cambridge, Department of Engineering, Trumpington Street, Cambridge CB2 1PZ, UK*

Hydrogenated amorphous silicon carbide films (a-SiC:H) were deposited using the electron cyclotron resonance chemical vapour deposition technique from a mixture of methane, silane and hydrogen, with diborane as the doping gas. The effect of the microwave power on the deposition rate were studied, and variations in the photo and dark conductivities were investigated in conjunction with film analysis using the Raman scattering technique. The conductivity increases rapidly to a maximum, followed by rapid reduction at high microwave powers. The ratio of the photo to dark conductivity,  $\sigma_{ph}/\sigma_d$ , peaks at microwave powers of  $\sim 600$  W. Under conditions of high hydrogen dilution and increasing microwave power, Raman scattering analysis showed evidence of the formation and increase of microcrystalline silicon and diamond-like components in the films, the former of which could account for the rapid increase and the latter the subsequent decrease in the conductivity.

## 1. Introduction

In recent years, there has been a growing interest in hydrogenated amorphous silicon carbide (a-SiC:H) thin films for applications in devices such as light-emitting diodes (LEDs), colour displays and solar cells. The majority of previous investigations into a-SiC:H films have concentrated on the use of the glow-discharge plasma-enhanced chemical vapour deposition (PECVD) technique using alkane sources such as CH<sub>4</sub>, C<sub>2</sub>H<sub>2</sub> and C<sub>2</sub>H<sub>4</sub> as carbon precursors and SiH<sub>4</sub> as the silicon source [1–3].

Doping of the a-SiC:H films has been achieved using a variety of techniques, such as the conventional PECVD [4, 5] and electron cyclotron resonance chemical vapour deposition (ECR-CVD) [6–8]. The advantage of the ECR-CVD method is that it is capable of producing a high excitation plasma which leads to a greater efficiency in the breaking of the C–H and Si–H bonds in the reactant gases. This has been reported to lead to a lower defect density and interfacial damage in the films deposited using this technique [9].

Kruangam *et al.* [6] and Hattori *et al.* [7] have previously reported the preparation of microcrystalline hydrogenated silicon carbide ( $\mu$ c-SiC:H) films at a low pressure of around 0.7 mtorr (1 torr = 133.322 Pa) using the ECR-CVD method.

The boron-doped films were reported to have the highest dark conductivity of around  $10 \Omega^{-1} \text{cm}^{-1}$  and optical bandgap of 2.25 eV. Mimura *et al.* [8] have also reported success in the deposition of n-type  $\mu$ c-SiC:H films at higher gas pressure (above 2.5 mtorr) using the ECR-CVD method. Both reports concluded that the gas pressure plays an important role in the film deposition characteristics using this technique. However, apart from these earlier reports by Hattori *et al.* and Kruangam *et al.*, there have been few reports on the deposition and characterization of p-type a-SiC:H films, especially using higher pressures in the ECR-CVD method.

In this paper, we report the deposition of boron-doped (p-type) a-SiC:H films at high pressures (of  $\sim 8$  mtorr) using the ECR-CVD method. In particular, the effect of changes in the microwave power on the deposition rate, conductivity (photo and dark) and the energy bandgap were investigated. A high hydrogen dilution was chosen during our depositions in order to investigate its effect on the microcrystallization process, because it has been reported that one of the key factors for the formation of microcrystalline components is the density of hydrogen radicals reaching the growing surface [6–8]. The Raman scattering technique was used to investigate this effect and the results are correlated with the conductivity data for

a probable explanation of the conductivity changes observed.

## 2. Experimental procedure

The schematic diagram of the ECR-CVD is shown in Fig. 1. The microwave power (2.45 GHz) is guided through a rectangular waveguide and introduced into the ECR magnetron excitation chamber through a quartz window. Using a current of 100 and 120 A for the upper and lower magnetic coils, respectively, a magnetic field of  $\sim 875$  G can be created within the excitation chamber. The magnetron controls a divergent-mirror magnetic-field profile that serves to extract the ECR plasma into the deposition chamber which is located below the excitation chamber. All the reactant gases (silane, methane and diborane) with the exception of hydrogen, are introduced into the deposition chamber. Hydrogen is introduced directly into the excitation chamber. The microwave ionizes the excitation gas to establish and maintain the plasma. During the deposition process, the total gas pressure in the chamber was maintained at  $\sim 8$  mtorr. The glass substrate (Corning 7059) was mounted on a heated stage in the deposition chamber below the aperture of the excitation chamber. For all depositions, the substrate temperature was maintained at  $230^\circ\text{C}$ .

The deposition conditions and film thicknesses are shown in Tables I and II, respectively. The hydrogen flow ratio (flows in standard  $\text{cm}^3 \text{min}^{-1}$ ) [hydrogen/silane + methane] is 98.7%, and the diborane ratio [diborane/silane + methane] is 2.5%. The film thickness was determined using a Dektak surface profiler. The optical bandgap was deduced from the transmittance and reflectance spectra of the films measured using a Perkin-Elmer UV/VIS spectrophotometer in the range 250–900 nm. The optical bandgap,  $E_0$ , of the film was determined from the Tauc's plot [10] by extrapolating the linear part of the absorption versus photon energy ( $h\nu$ ) curve.

The d.c. conductivity was measured on a planar configuration with pre-evaporated aluminium contacts 1 cm wide and 1 mm apart. A computer-controlled Keithley source-measure unit system was used for the current-voltage (I-V) measurements. Symmetrical I-V curves confirm the ohmic nature of the contacts.

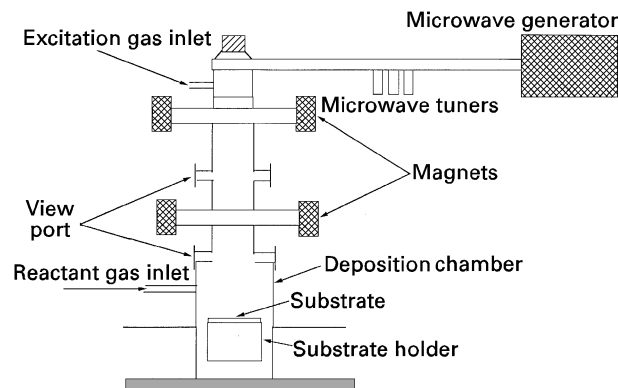


Figure 1 Schematic diagram of the ECR-CVD deposition system.

TABLE I Summary of deposition conditions

Substrate temperature	230 °C	
Total gas pressure	8 mtorr	
Microwave power	150–900 W	
Excitation gas	H <sub>2</sub>	56 standard cm <sup>3</sup> min <sup>-1</sup>
Reactant gases	SiH <sub>4</sub> (10% in H <sub>2</sub> )	6 standard cm <sup>3</sup> min <sup>-1</sup>
	CH <sub>4</sub>	0.6 standard cm <sup>3</sup> min <sup>-1</sup>
	B <sub>2</sub> H <sub>6</sub> (500 p.p.m. in H <sub>2</sub> )	60 standard cm <sup>3</sup> min <sup>-1</sup>

TABLE II Sample identification and SiC:H film thickness

Sample	Microwave power (W)	Film thickness (nm)
1	150	285.8
2	350	253.2
3	500	263.4
4	550	248.5
5	600	251.5
6	650	264.5
7	700	278.9
8	800	240.1
9	900	272.0

A fibre optic light source supplied from a 400 W Xenon lamp was used for illumination during the photoconductivity measurements. The Raman scattering measurements were performed at room temperature using the 514.5 nm line of a CW argon-ion laser. The back scattered signals were analysed using a high-resolution double-pass monochromator and detected using a cooled GaAs photomultiplier detector. The microwave power was varied from 150–900 W to investigate its influence on the film characteristics.

## 3. Results and discussion

Fig. 2 shows the variation in the film deposition rate as a function of the microwave power. It can be seen that the deposition rate increases to its maximum value at a microwave power of 500 W, and then decreases. A reasonable explanation is the competition between deposition and ion etching. At low microwave power, the hydrogen-ion etching effect is relatively weak and the deposition effect is dominant, with the reaction species created by the plasma increasing with increase in the microwave power. However, at higher microwave powers, greater ionization of the hydrogen occurs, resulting in greater ion energy which can lead to an enhanced etching effect; hence a reduction in the film thickness. As described previously, the optical bandgap,  $E_0$ , of the film was calculated from the Tauc's plot. For comparison, an alternative method [11] in which the bandgap is defined as the energy at which the absorption coefficient equals  $10^4 \text{ cm}^{-1}$  ( $E_{0.4}$ ) was also used. It was determined that both the  $E_0$  and the  $E_{0.4}$  bandgaps did not change very significantly with changes in the microwave power.

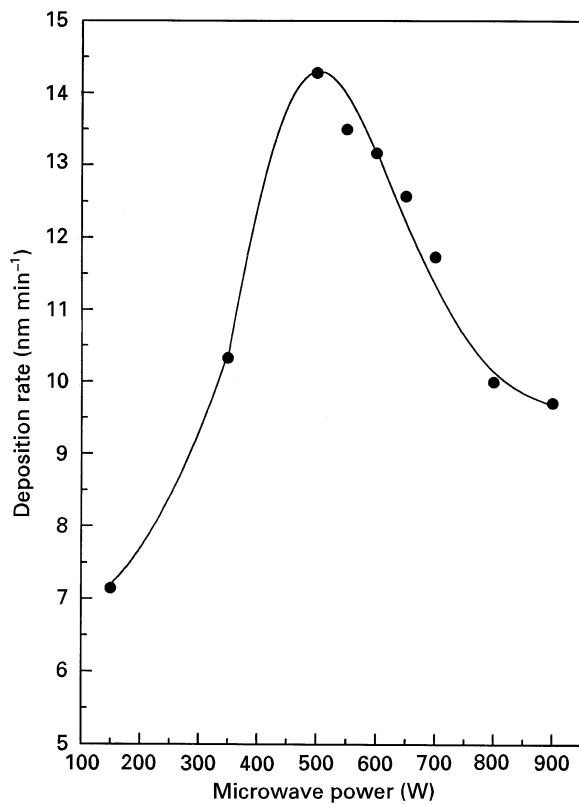


Figure 2 Plot of deposition rate as a function of the microwave power showing maximum deposition rate at a microwave power of  $\sim 500$  W.

The  $E_0$  values varied between 1.9 and 2.1 eV, and the  $E_{0.4}$  values varied between 2.0 and 2.2 eV. In both cases, no particular trend of variation with the microwave power was observed. Consistent with a report by Solomon *et al.* [12], the optical bandgap values derived using the  $E_{0.4}$  method are always higher compared to the  $E_0$  values calculated from the Tauc's plot. In the case of our samples, the ratio of  $E_0/E_{0.4}$  equals  $\sim 0.8$ .

A significant change in the photo and dark conductivity was observed as the microwave power was increased, as shown in Fig. 3. The conductivity increases considerably with the maximum value achieved at a microwave power of  $\sim 700$  W, beyond which it decreases rapidly. A similar trend of conductivity change was also reported by Hattori *et al.* [7] who achieved the highest conductivity at a microwave power of 300 W in p-type samples deposited at a low total pressure of 0.7 mtorr, suggesting that higher microwave powers are required to achieve a conductivity change at higher gas pressures.

The Raman scattering results in Fig. 4 show that the dominant peak shifts from  $\sim 460$   $\text{cm}^{-1}$  to  $480$   $\text{cm}^{-1}$  (due to the amorphous nature) to  $\sim 520$   $\text{cm}^{-1}$  (corresponding to the transverse-optic-like mode of crystalline silicon) as the microwave power is increased, suggesting that a probable cause of the conductivity increase could be the formation of microcrystalline silicon components in the film in addition to the amorphous state. In these samples, the carbon atoms in the microcrystalline SiC film probably reside in the amorphous material that is interposed between the

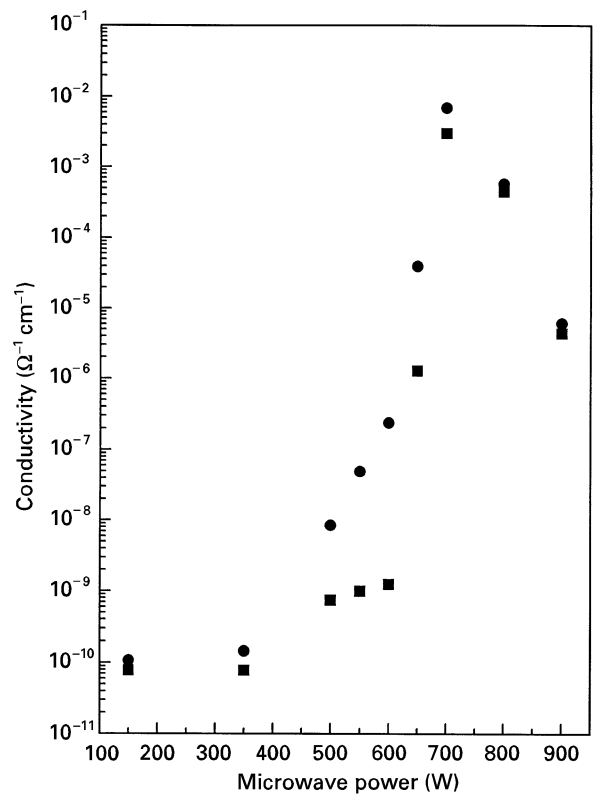


Figure 3 Plot of conductivity, (●) photo, (■) dark, as a function of the microwave power showing maximum conductivity at a microwave power of  $\sim 700$  W.

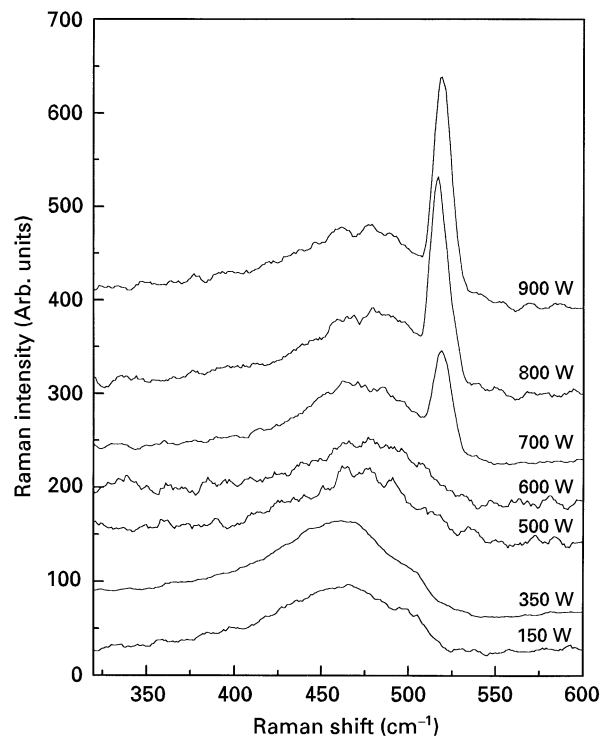


Figure 4 Raman spectra of samples deposited at microwave powers from 150–900 W showing the evolution of the microcrystalline silicon signal at  $\sim 520$   $\text{cm}^{-1}$  in samples deposited at microwave powers exceeding  $\sim 600$  W.

silicon microcrystallites. The degree of crystallization which can be estimated from the relative ratio of the Raman signal at  $520$   $\text{cm}^{-1}$  to that at between  $460$  and  $480$   $\text{cm}^{-1}$  is lower at lower microwave powers. In

samples deposited at below 700 W, no signals corresponding to microcrystalline silicon ( $520\text{ cm}^{-1}$ ) were detected in the Raman spectra, in agreement with the reports by Demichelis *et al.* [5] and Wang *et al.* [4] in samples deposited using the PECVD method. Fig. 5 shows the Raman spectra beyond  $600\text{ cm}^{-1}$  of the samples deposited at 700, 800 and 900 W, respectively. The spectra show the evolution of spectral features (strongest in the case of the sample deposited at 900 W) associated with what appeared to be diamond-like components in the range  $1200\text{--}1450\text{ cm}^{-1}$ . It was shown earlier that samples deposited at microwave powers of 800 and 900 W have exhibited a sharp reduction in the conductivity, an effect which is probably related to the presence of these diamond-like components.

The results in Fig. 3 are plotted in Fig. 6 as the ratio of photo to dark conductivity ( $\sigma_{\text{ph}}/\sigma_{\text{d}}$ ) as a function of the microwave power. The peak ( $\sigma_{\text{ph}}/\sigma_{\text{d}}$ ) of  $\sim 200$  occurred at  $\sim 600\text{ W}$ . At this microwave power, the Raman scattering spectra in Fig. 4 indicate a transformation from the amorphous state towards the mixed amorphous/microcrystalline state. This suggests that the highest photosensitivity ( $\sigma_{\text{ph}}/\sigma_{\text{d}}$ ) occurs when the films are in transformation between amorphous and microcrystalline embedded in the amorphous matrix. In the absence of transmission electron microscopy (TEM) data in the present study, the exact nature of the material characteristics which give rise to this sharp change in the photosensitivity, is presently unknown, and warrants further investigation.

The presence of non-emissive radicals [8] in the high gas-pressure regime, contributes largely to the surface coverage and affects the nucleation mecha-

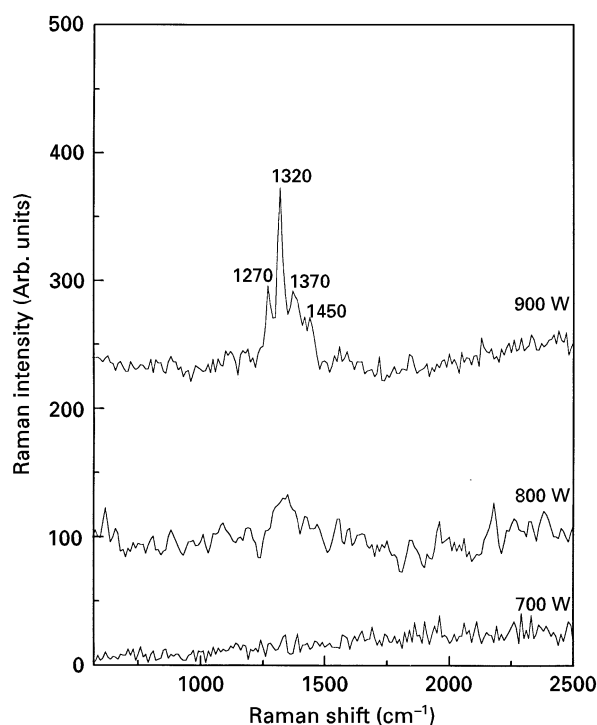


Figure 5 Raman spectra beyond  $600\text{ cm}^{-1}$  of the samples deposited at 700–900 W showing the evolution of spectral features (strongest in the case of the sample deposited at 900 W) associated with what appeared to be diamond-like components in the range  $1200\text{--}1450\text{ cm}^{-1}$ .

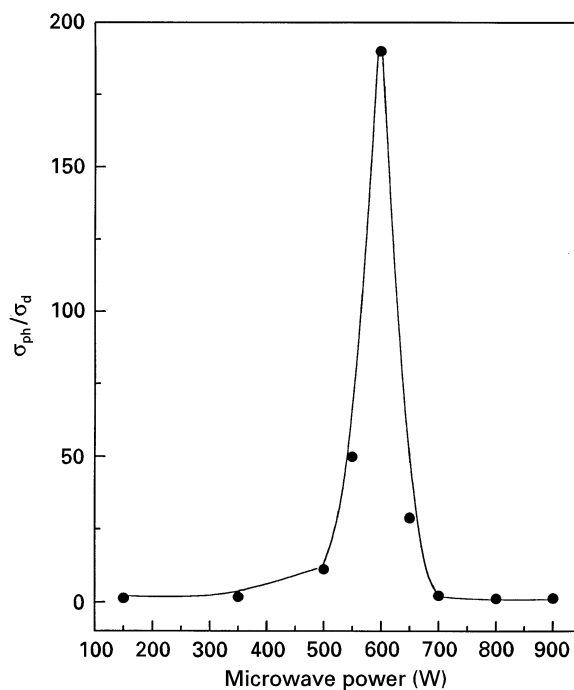


Figure 6 Plot of photosensitivity,  $\sigma_{\text{ph}}/\sigma_{\text{d}}$ , as a function of the microwave power showing maximum sensitivity at a microwave power of  $\sim 600\text{ W}$ .

nism. The result of this is to help ease the formation of microcrystals in the film. However, the presence of boron has been reported [5] to inhibit the microcrystalline formation process, unlike phosphine which has the reverse effect of enhancing this process [5]. In our case, at higher gas pressures, the number of non-reactive boron species reaching the growing surface is expected to be large, thus possibly leading to a greater inhibition effect on the microcrystalline formation process. Therefore, unlike in the reports by Hattori *et al.* [7], higher microwave powers are thus required to achieve microcrystalline formation.

#### 4. Conclusion

Results from the bandgap, conductivity and Raman scattering characterization of boron-doped a-SiC:H films deposited using the ECR-CVD method, are reported. The effect of changes in the microwave power on the optical bandgap, photo and dark conductivities as well as the Raman spectra were investigated. There is analytical evidence from the Raman spectra to suggest a transformation from a-SiC:H to  $\mu\text{c-SiC:H}$  at increasing microwave power. Both the photo and dark conductivities were observed to increase rapidly following the formation of the microcrystalline components embedded in the amorphous matrix of the films. At higher microwave powers exceeding  $\sim 700\text{ W}$ , the Raman spectra show evidence of the presence of diamond-like components which could have contributed to the observed rapid reduction in both the photo and dark conductivities. The photosensitivity ( $\sigma_{\text{ph}}/\sigma_{\text{d}}$ ) was found to be the highest when the films are in transformation from the amorphous state to the mixed amorphous/microcrystalline state. The optical bandgap does not change significantly with changes in the microwave power, suggesting that

these microcrystalline inclusions are probably small and therefore their effect on the optical bandgap is negligible.

### Acknowledgements

The authors are grateful to the Nanyang Technological University and to the School of Electrical and Electronic Engineering for the support of this work. This project was carried out in collaboration with the Engineering Department of the University of Cambridge under the NTU-CUED collaboration programme. The technical assistance of Dr L. H. Chua, Dr D. H. Zhang, M. Shamsul and T. H. Foo is gratefully acknowledged.

### References

1. M. N. P. CARRENO, I. PEREYRA, M. C. A. FANTINI, H. TAKAHASHI and R. LANDERS, *J. Appl. Phys.* **75** (1994) 538.
2. S. Z. HAN, H. M. LEE and H. S. KWON, *J. Non-Cryst. Solids* **170** (1994) 199.

3. F. DEMICHELIS, G. CROVINI, F. GIORGIS, C. F. PIRRI and E. TRESSO, *Diamond Rel. Mater.* **4** (1995) 473.
4. C. WANG, G. LUCOVSKY and R. J. NEMANICH, *Proc. Mater. Res. Soc. Symp.* **219** (1991) 751.
5. F. DEMICHELIS, C. F. PIRRI and E. TRESSO, *J. Appl. Phys.* **72** (1992) 1327.
6. D. KRUANGAM, T. TOYAMA, Y. HATTORI, M. DEGUCHI, H. OKAMOTO and Y. HAMAKAWA, *J. Non-Cryst. Solids* **97/98** (1987) 293.
7. Y. HATTORI, D. KRUANGAM, T. TOYAMA, H. OKAMOTO and Y. HAMAKAWA, *ibid.* **97/98** (1987) 1079.
8. H. MIMURA, T. FUTAGI, T. MATSUMOTO, M. KATSUNO, Y. OHTA and K. KITAMURA, *Appl. Surf. Sci.* **65/66** (1993) 473.
9. T. MIYAJIMA, K. SASAKI and S. FURUKAWA, in "Proceedings of the 4th International Conference on Amorphous and Crystalline Silicon Carbide" (Springer-Verlag, Berlin, Germany, 1992) p. 281.
10. J. TAUC, in "Amorphous and Liquid Semiconductors" edited by J. Tauc (Plenum, New York, 1974) Ch. 4.
11. R. A. STREET, *Philos. Mag.* **B37** (1978) 35.
12. I. SOLOMON, M. P. SCHMIDT and H. TRAN-QUOC, *Phys. Rev.* **B38** (1988) 9895.

*Received 23 February  
and accepted 31 July 1996*